

## Partially isolated four port converter with combined PWM and secondary phase shift control

G. Ranipriya, R. Jegatheesan, K. Vijayakumar

Department of Electrical and Electronics Engineering, SRM Institute of Science and Technology, Kancheepuram, India

---

### Article Info

#### Article history:

Received Jan 22, 2020

Revised Aug 6, 2020

Accepted Sep 23, 2020

---

#### Keywords:

DC-DC converters

Multiport converters

PWM control

Renewable energy sources

---

### ABSTRACT

A partially isolated four-port converter is proposed in this paper for interfacing two renewable sources and a storage device with an isolated load. This converter is capable of achieving high power density because of the effective sharing of devices among the input ports. Combined PWM and secondary phase shift control is employed to have a decoupled power flow management of input and output side ports. PWM control is used at the input side for maximum power tracking of renewable sources and battery power management. At the output side, secondary Phase shift control is used for controlling the output voltage. The adopted secondary phase shift control allows the primary switching legs to be operated with 180° phase shift which results in reduced current ripple at input ports. The working principle of the converter, its output characteristics and control strategy are discussed. Working of the converter and its control strategy is verified through simulation for different input and output conditions. Further, to validate the simulation results, the experimental results of a 500 W prototype are also provided.

*This is an open access article under the [CC BY-SA](https://creativecommons.org/licenses/by-sa/4.0/) license.*



---

### Corresponding Author:

K. Vijayakumar

Department of Electrical and Electronics Engineering

SRM Institute of Science and Technology

Kancheepuram, Tamil Nadu, India

Email: kvijay\_srm@rediffmail.com

---

## 1. INTRODUCTION

Recently there is an increased penetration of renewable energy generation systems in various fields such as spacecraft power supplies, electric vehicles, and micro-grids. The use of more than one energy source with energy storage element becomes necessary in renewable power generation systems to ensure continuous supply to the load or grid, despite their intermittent nature [1-3]. For interfacing, multiple renewable energy sources and storage with the load or grid, either several individual two-port converters or a single multiport converter can be used. The multiport set-up is preferable due to its reduced size and cost, high power density, high efficiency and centralized control features [4-6].

Various topologies of multiport converters, including non-isolated multiport [7-9], fully-isolated multiport [10-12] and partially-isolated multiport [13-16] topologies are reported in many works of literature. Non-isolated topologies have a compact structure and are mostly developed from the fundamental buck, boost and buck/boost circuits. The limitations of these topologies are that attaining ZVS in switching devices is complex and widely varying voltage levels at source ports cannot be interfaced. Fully-isolated topologies allow wide voltage variations at the ports by employing a multi-winding transformer. These topologies are derived from half or full bridge converters and almost all active switches achieve ZVS. The use of so many active devices without any sharing makes the system more complex and reduces the power density. Partially-isolated topologies are derived by integrating non-isolated converters with isolated converters. These topologies

achieve high power density, with a compact structure. In these topologies, a single winding transformer is used for providing necessary isolation with flexible voltage handling capability at the load port, while the primary sources and storage ports are not isolated.

Many partially-isolated multiport topologies have been reported in works of literature because of their remarkable advantages. Some boost integrated full-bridge three-port converters derived by integrating non-isolated boost converters with isolated full-bridge phase-shifted converters have been proposed in [17-20] and four-port converters in [21, 22]. In all these converters phase shifting at primary side is employed, i.e., for tracking the maximum power point of the sources and for battery management, the PWM control of the switches at primary side switching legs are used and the phase shift between the switching pulses of the same primary side switching legs are used for output regulation. Hence in primary phase shift control, the decoupling of power control loops becomes difficult, and the voltage of all the ports are happened to be regulated by the same control variable and duty cycle of primary side switches which increases the control difficulty. Similar to the primary side phase-shifted two-port converters, multiport converters also have the limitations of higher current ripple at input ports and higher conduction losses due to the current circulation at the free-wheeling interval, low duty cycle utilization and more recovery losses due to diodes of the secondary-side rectifier.

The secondary phase-shift control technique has been introduced to overcome the above said drawbacks of primary phase shifting, and have applied to several single-input single-output converters [23-25]. In this paper, a partially isolated four-port converter with combined PWM and secondary phase-shifting control is introduced by adding controllable switches to the secondary side. In this combined PWM and secondary phase-shift control, the PWM control of the primary side switches is used for maximum power tracking and battery power management. And the difference in switching instants of primary and secondary side switches called as phase shift is used for controlling the output voltage. The control variables that determines the duty cycles of the input side boost converters only depends on the voltages and currents of sources or battery and not on the output voltage. This decoupling of the control variables of the phase shift and duty cycle simplifies the difficulty in control and decouples the power flow control of input and output ports. Also, due to the secondary side phase-shifting strategy, the primary side switches can be operated with 180° phase shift (like interleaving), which results in a reduction of ripple currents at input ports and improves duty cycle usage of primary switches.

## 2. PROPOSED PARTIALLY ISOLATED FOUR-PORT CONVERTER

### 2.1. Circuit description

The proposed partially isolated four-port converter with combined PWM and secondary side phase-shifted control is shown in Figure 1. It is applied for connecting two PV sources and a battery to a standalone dc-load. The MOSFETs S1 and S2 and inductor L1 form a boost converter, connecting source PV1 and the battery. While MOSFETs S3 and S4 and inductor L2 form another boost converter connecting source PV2 and battery. Thus from PV to the battery, the proposed converter works as a boost converter. A dc blocking capacitor CB is introduced between the phase legs to compensate for the differences in voltage across the switching legs, which arises due to the asymmetrical operation caused by the difference in duty cycles. The output port is isolated from the source and storage ports through a high-frequency transformer. To the secondary of high-frequency transformer, a full bridge active rectifier with four controllable MOSFET switches S5-S8 is connected. From battery to load port, the converter works as an isolated full-bridge converter with secondary side phase shifting. Lx is the leakage inductance of the high-frequency transformer and the required external inductance which determines the maximum power transferred between the primary and secondary sides. Here, the primary side switches are shared by both boost and phase-shifted converters thus reducing the component count and increases the power density.

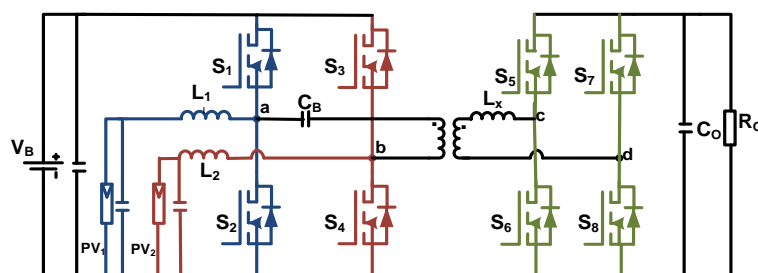


Figure 1. Proposed partially isolated four-port converter

**2.2. Working of boost converters**

The section of the converter from the PV sources to the battery is equivalent to two boost converters. The waveforms depicting the operation of the boost converters are shown in Figure 2. Inductor  $L_1$  gets charged when  $S_2$  is ‘on’ and when  $S_1$  is ‘on’ it gets discharged. Similarly, the inductor  $L_2$  gets charged when  $S_4$  is ‘on’ and when  $S_3$  is ‘on’ it gets discharged. The power flow between the sources ( $PV_1$  and  $PV_2$ ) and the battery is controlled by duty cycles of the corresponding switches  $S_2$  and  $S_4$ . The tracking of the maximum power of the PV sources is also achieved through duty cycle control of the switching devices. The voltage transfer ratio of the boost converter section is given by,

$$V_B = \frac{V_{PV1}}{1-D_1} = \frac{V_{PV2}}{1-D_2} \tag{1}$$

where  $V_B$  is the voltage at battery port,  $V_{PV1}$  and  $V_{PV2}$  are the voltages at PV ports,  $D_1$  and  $D_2$  are the duty ratios of the boost converter one and two respectively.

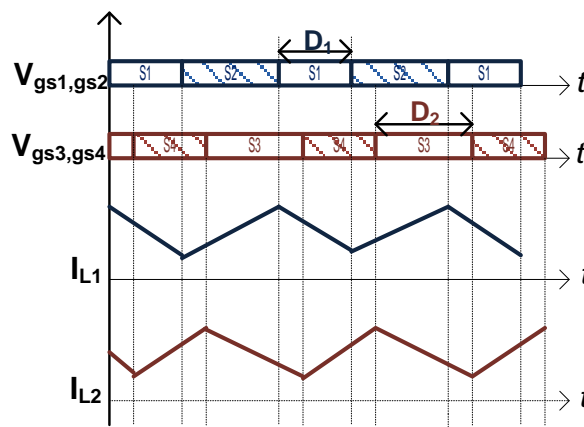


Figure 2. Operational waveforms of primary side boost converters

**2.3. Working of full bridge secondary side phase shifted converter**

The section of the converter from the battery to the load is equivalent to a secondary phase-shifted full-bridge converter. The voltage conversion ratio ( $m$ ) of this section is given as,

$$m = \frac{V_O}{nV_B} \tag{2}$$

where  $V_O$  is the voltage of output port and  $n$  is the turn’s ratio of the high-frequency transformer.

The load conditions of the output port determine the shape of the secondary side inductor current. For heavy load conditions, the secondary side inductor current will be continuous and for light load conditions, it will be discontinuous. Operational analysis for continuous current conduction mode is given in the following section. For analysis, it is considered that a switching cycle consists of five intervals and the circuit representing the state of the converter in each interval is shown in Figure 3 and waveforms related to each interval are shown in Figure 4. ‘ $V_{AB}$ ’ and ‘ $V_{CD}$ ’ are the voltages of primary and secondary bridges respectively. ‘ $\phi$ ’ (angle of phase shift) is used to represent the difference in switching instants of input side switches and the corresponding output side switches. By adjusting this phase angle, the power transfer from the primary to the secondary side is controlled.

Interval I [ $t_0-t_1$ ]: MOSFET switch  $S_1$  is turned ‘on’ at the time ‘ $t_0$ ’ and its body diode will be conducting due to the current flowing through inductor  $L_X$ , achieving zero voltage turn-on.  $S_4$ ,  $S_6$ , and  $S_7$  remain ‘on’. The secondary side inductor current,  $I_{LX}$  increases linearly and reaches its peak at time ‘ $t_1$ ’, ending the switching state. The change in inductor current is given by,

$$\frac{dI_{LX}}{dt} = \frac{nV_B+V_O}{L_X} \tag{3}$$

$$I_{Lx}(t) = \frac{nV_B+V_0}{L_x}(t - t_0) + I_{Lx}(t_0); \quad t_0 \leq t < t_1 \tag{4}$$

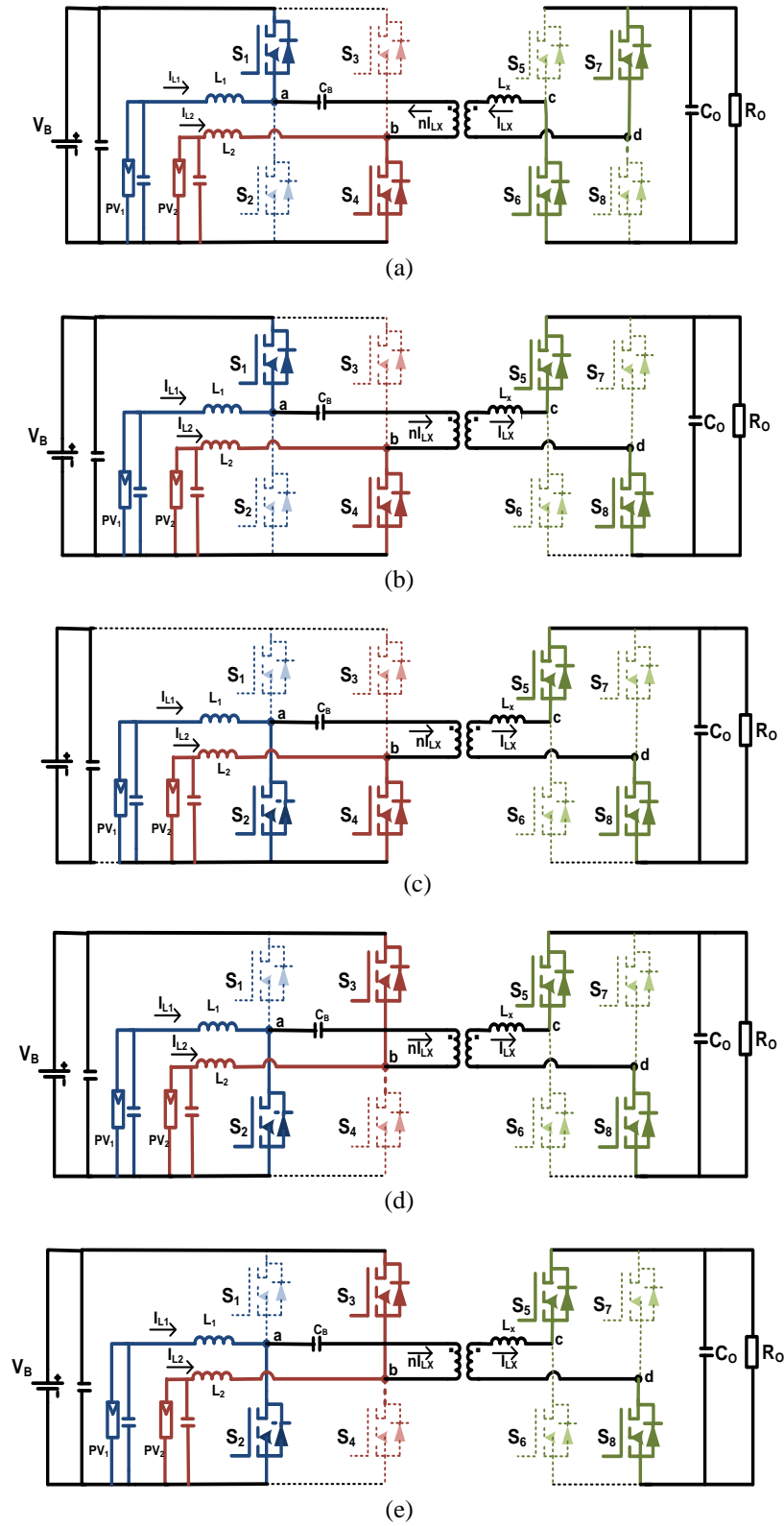


Figure 3. Equivalent circuits in continuous conduction mode, a) interval-i ( $t_0-t_1$ ), b) interval-ii ( $t_1-t_2$ ), c) interval-iii ( $t_2-t_3$ ), d) interval-iv ( $t_3-t_4$ ), e) interval-v ( $t_4-t_5$ )

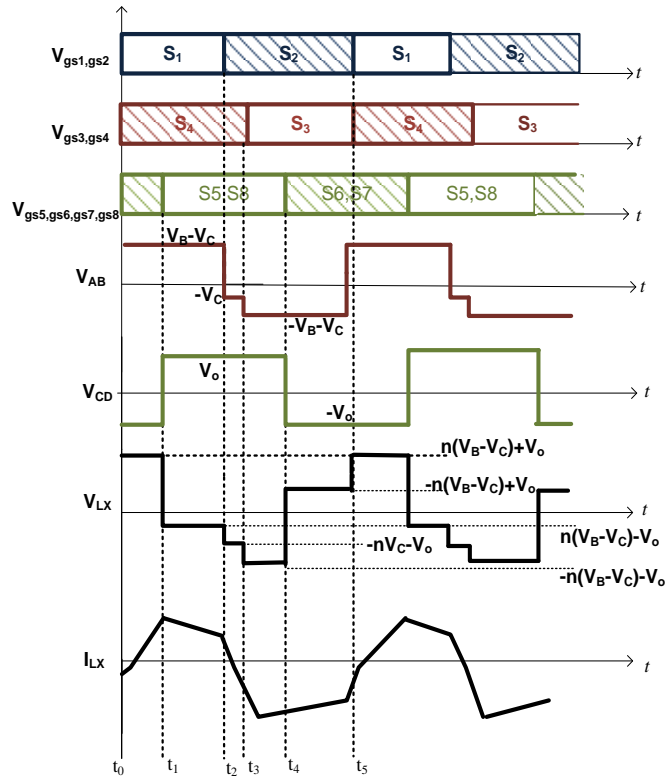


Figure 4. Waveforms of secondary side phase-shifted converter

Interval II [t<sub>1</sub>-t<sub>2</sub>]: At time ‘t<sub>1</sub>’, the secondary side switches S<sub>5</sub> & S<sub>8</sub> turn ‘on’, the current through the inductor L<sub>x</sub>, discharges, delivering power to the load. Thus,

$$\frac{dI_{Lx}}{dt} = \frac{nV_B - V_O}{L_x} \tag{5}$$

$$I_{Lx}(t) = \frac{nV_B - V_O}{L_x}(t - t_1) + I_{Lx}(t_1); \quad t_1 \leq t < t_2 \tag{6}$$

Interval III [t<sub>2</sub>-t<sub>3</sub>]: At time ‘t<sub>2</sub>’, MOSFET switch S<sub>1</sub> turns ‘off’ while S<sub>2</sub> turns ‘on’. S<sub>4</sub>, S<sub>5</sub>, S<sub>8</sub> remain ‘on’. The secondary side inductor discharges, delivering power to the load in this interval. Hence,

$$\frac{dI_{Lx}}{dt} = \frac{-V_O}{L_x} \tag{7}$$

$$I_{Lx}(t) = \frac{-V_O}{L_x}(t - t_2) + I_{Lx}(t_2); \quad t_2 \leq t < t_3 \tag{8}$$

Interval IV [t<sub>3</sub>-t<sub>4</sub>]: While MOSFET switch S<sub>4</sub> turns off at time ‘t<sub>3</sub>’, S<sub>3</sub> turns ‘on’ with ZVS. The switches S<sub>2</sub>, S<sub>5</sub>, S<sub>8</sub> remain conducting. The voltage across the inductor L<sub>x</sub> will be negative which results in a linear decrease of current (I<sub>Lx</sub>) through it. Thus,

$$\frac{dI_{Lx}}{dt} = \frac{-nV_B - V_O}{L_x} \tag{9}$$

$$\frac{-nV_B - V_O}{L_x}(t - t_3) + I_{Lx}(t_3); \quad t_3 \leq t < t_4 \tag{10}$$

Interval V [t<sub>4</sub>-t<sub>5</sub>]: At time ‘t<sub>4</sub>’, the secondary side switches S<sub>5</sub> and S<sub>8</sub> goes to ‘off’ state while S<sub>6</sub> and S<sub>7</sub> turn ‘on’. The switches S<sub>2</sub>, S<sub>3</sub> at the primary side keep conducting. The current through the inductor I<sub>Lx</sub> reverses and increases in the opposite direction. Thus,

$$\frac{dI_{Lx}}{dt} = \frac{-nV_B + V_o}{L_x} \tag{11}$$

$$I_{Lx}(t) = \frac{-nV_B + V_o}{L_x} (t - t_4) + I_{Lx}(t_4); t_4 \leq t < t_5 \tag{12}$$

**2.4. Output characteristics**

For deriving the expression for output voltage, the average current of the secondary side inductor is considered,

$$I_{avg} = \frac{1}{2f_s L_{hf}} \varphi(1 - \varphi)V_o \tag{13}$$

The supplied input power is,

$$P_{in} = nV_B I_{avg} = \frac{nV_B V_o}{2\pi^2 f_s L_x} \varphi(\pi - \varphi) \tag{14}$$

Output power is  $P_o = \frac{V_o^2}{R_L}$ ,

Neglecting the transformer and switching losses and considering  $P_o = P_{in}$ ,

The output voltage is given by,

$$V_o = \frac{nV_B}{2\pi^2 f_s L_x} R_L \varphi(\pi - \varphi) \tag{15}$$

The output power is given by,

$$P_o = \left( \frac{nV_B}{2\pi^2 f_s L_x} \right)^2 \varphi^2(1 - \varphi)^2 R_L \tag{16}$$

From the output voltage and power equations, it can be inferred that the output voltage and power is the function of phase shift alone and not on the duty cycles of primary side switches.

**3. PROPOSED CONTROL METHOD**

The combined PWM and secondary phase-shifting control is employed for power management of ports and is shown in Figure 5. Four control loops are employed for tracking the maximum power of two PV sources, charging and discharging control of battery and regulation of load. At PV ports, voltages and currents are sensed and maximum power tracking is achieved through MPPT control loops. In the battery port, constant current charging and constant voltage charging control are achieved with battery current (BCC) and battery voltage (BVC) control loops. For primary side control, the minimum of the control variables coming from the MPPT and battery regulator blocks are used for generating duty cycles D1 and D2 for the primary side switches. For MPPT widely used Perturb and observe algorithm is used to generate the duty cycles. The output voltage regulation (OVR) control loop employs a simple voltage control technique, where the voltage at the output is sensed to calculate the corresponding phase-shift required between the switching instants of primary and secondary switches.

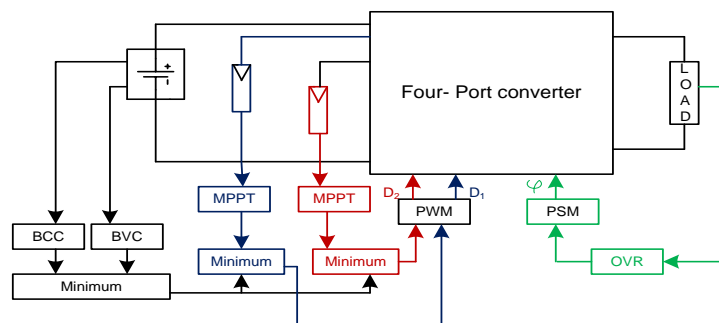


Figure 5. Combined PWM and secondary side phase-shifting control

Here, the currents and voltages at PV and battery ports determine the duty cycles D1 and D2. The output voltage determines the phase-shift between the primary and secondary switches. The voltage at the output port doesn't have any impact in the process of duty cycle determination. Thus power control of input ports is decoupled from output ports.

#### 4. RESULTS AND DISCUSSIONS

Simulation is carried out for verifying the working principle of the proposed four-port converter and its control structure using the following parameters: Battery voltage ( $V_B=80$  V), PV voltages=30-40 V, Load voltage=100-120 V, Load power=0-500 W, switching frequency=10 KHz, Transformer turns ratio=1.5, secondary side inductor ( $L_X=60.61$   $\mu$ H), Boost inductors=0.49 mH, Blocking capacitor ( $CB=15$   $\mu$ f). In Figure 6, the steady-state inductor current waveforms of the buck/boost converters at the primary side are shown. The midpoint voltages from the switching legs of input and output side bridges and the corresponding load voltage waveform for that phase-shift are given in Figure 7.

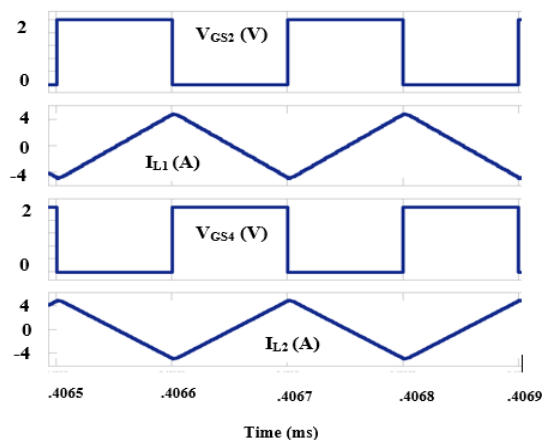


Figure 6. Gate pulses and boost inductor current waveforms

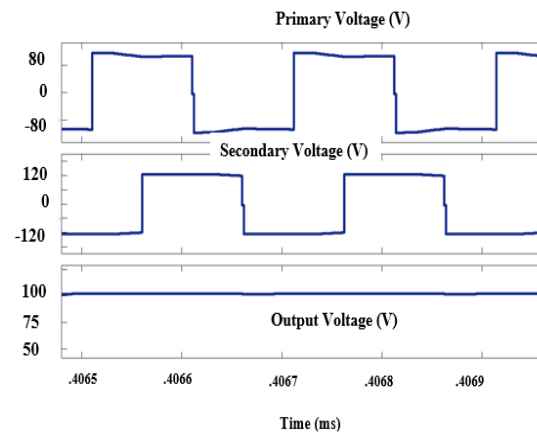


Figure 7. Phase-shifted voltages and output voltage

Further simulation is performed by varying power levels of different ports and the observations are listed in Table 1 and Table 2. It is evident from Table 1, that the variations in power generated by PVs have no effect on the output voltage as the duty cycle control loop and output voltage regulator loop are decoupled from each other. And from Table 2, it is evident that the load changes does not have any effect on PV power but only on battery power, which ensures that the control loops for phase-shifting and duty cycle are decoupled from one other. Thus the output regulation can be done simultaneously while tracking the maximum power of PVs, by adjusting the battery power.

Table 1. Power at different ports when load power is constant

	SISO	DI	DO
PPV1+ PPV2 (W)	0	360	600
PB(W)	500	140	-100
Po(W)	500	500	500

Table 2. Power at different ports when PV power remains constant

	SISO	DI	DO
PPV1+ PPV2 (W)	300	300	300
PB (W)	80	125	-100
Po (W)	380	425	200

After verifying the working of the four-port converter with simulation, a prototype model of 500 W rating shown in Figure 8 has been built for further validation of the analysis and simulation. The inductor currents of boost converter section at steady state with the gate pulse are shown in Figure 9. In Figure 10, primary and secondary phase-shifted voltages and the corresponding output voltage at steady state are given. From Figure 11, it is clear that for load changes, there is only a change in battery current and not in output voltage. Figure 12 shows that current from PV1 is constant and PV2 decreases, for this change the battery is compensating by discharging. The experimental results match the simulation results pretty well.

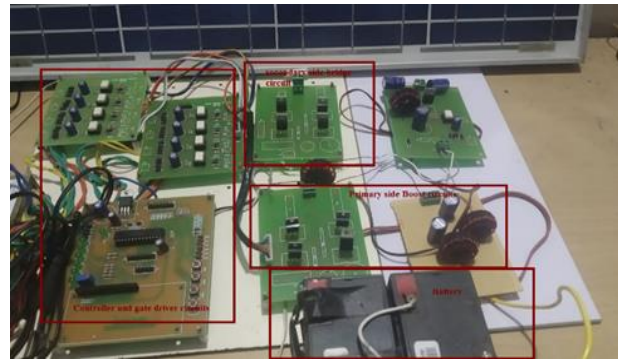


Figure 8. The prototype of four-port converter

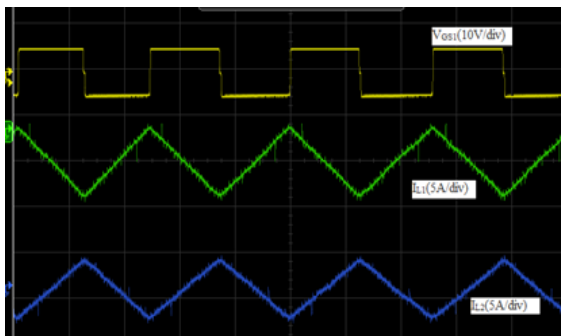


Figure 9. Current waveforms of boost inductors at the primary side

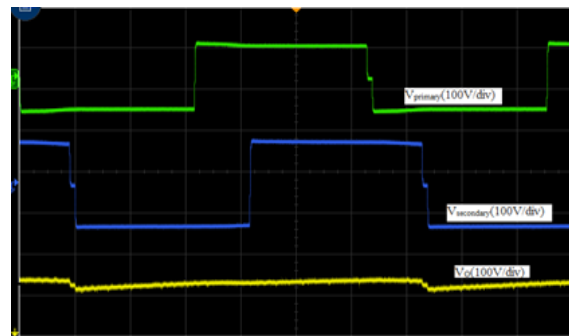


Figure 10. Phase-shifted voltages from the primary and secondary bridge

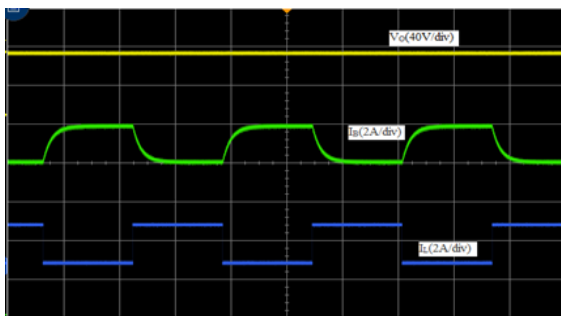


Figure 11. Battery current variations for load current

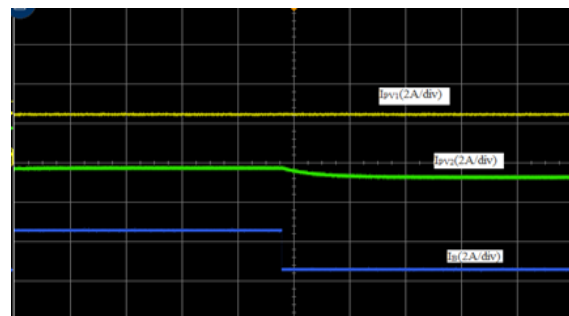


Figure 12. Battery current variations for PV current variations

### 5. CONCLUSION

A partially isolated four-port converter, employing combined PWM and secondary phase-shifting control has been developed and applied for connecting two PV sources and a battery to a dc-load. This converter has the advantage of simplified structure and higher power density due to the effective sharing of components among the input ports. The complexity in control of the converter also has been reduced due to the adoption of combined PWM and secondary phase-shifting control technique. This control technique effectively decouples control variables of the duty cycle and phase-shift and provides an independent power flow control of input and output ports. Also, the current ripple at the PV ports of the two boost converters is reduced significantly in the secondary phase-shift control technique than primary phase-shift control. The working principle of the converter and its output characteristics and control strategy were discussed. Simulation and experimental results demonstrate the working of the proposed converter and the feasibility of its control strategy for different operating conditions. Thus, the proposed converter can be applied for renewable energy based stand-alone or micro-grid applications due to its remarkable merits.

## REFERENCES

- [1] W. Jiang and B. Fahimi, "Multiport Power Electronic Interface-Concept, Modeling, and Design," *IEEE Transactions on Power Electronics*, vol. 26, no. 7, pp. 1890-1900, 2011.
- [2] L. I. Yunwei, and F. Nejabatkhah, "Overview of control, integration and energy management of microgrids," *Journal of Modern Power Systems and clean energy*, vol. 2, no. 3, pp. 212-222, 2014.
- [3] N. Zhang, D. Sutanto, K. M. Muttaqi, "A review of topologies of three-port DC-DC converters for the integration of renewable energy and energy storage system," *Renewable and Sustainable Energy Reviews*, vol. 56, pp. 388-401, 2016.
- [4] J. Zeng, W. Qiao, and L. Qu, "An isolated multiport DC-DC converter for simultaneous power management of multiple renewable energy sources," in *2012 IEEE Energy Conversion Congress and Exposition (ECCE)*, Raleigh, NC, 2012, pp. 3741-3748.
- [5] G. Ranipriya and K. Vijayakumar, "A Brief Review on Partially Isolated Bidirectional Multiport Converters for renewable energy sourced DC Microgrids," *International journal of renewable energy research*, vol. 10, no. 2, pp. 601-613, 2020.
- [6] J. Zeng, W. Qiao, L. Qu, and Y. Jiao, "An Isolated Multiport DC-DC Converter for Simultaneous Power Management of Multiple Different Renewable Energy Sources," *IEEE Journal of Emerging and Selected Topics in Power Electronics*, vol. 2, no. 1, pp. 70-78, 2014.
- [7] H. Matsuo, Wenzhong Lin, F. Kurokawa, T. Shigemizu and N. Watanabe, "Characteristics of the multiple-input DC-DC converter," *IEEE Transactions on Industrial Electronics*, vol. 51, no. 3, pp. 625-631, 2004.
- [8] H. Wu, Y. Xing, Y. Xia, K. Sun, "A family of non-isolated three-port converters for stand-alone renewable power system," *IECON 2011-37th Annual Conference of the IEEE Industrial Electronics Society*, Melbourne, VIC, 2011, pp. 1030-1035.
- [9] Prabhala. V. A., Fajri P., Gouribhatla V. S., Prashant B., Baddipadiga, Mehidi F., "A DC-DC converter with High Voltage gain and Two Input Boost stages," *IEEE Transactions on Power Electronics*, vol. 31, no. 6, pp. 4206-4216, 2015.
- [10] H. Tao, J. L. Duarte, and M. A. M. Hendrix, "Three-Port Triple-Half-Bridge Bidirectional Converter With Zero-Voltage Switching," *IEEE Transactions on Power Electronics*, vol. 23, no. 2, pp. 782-792, 2008
- [11] A. Ajami and P. Shayan, "Soft-switching method for multiport DC/DC converters applicable in grid-connected clean energy sources," *IET Power Electronics*, vol. 8, no. 7, pp. 1246-1254, 2015.
- [12] Wang Z. and Li H., "An integrated three-port bidirectional DC-DC converter for PV application on a DC distribution system," *IEEE Transactions on Power Electronics*, vol. 28, no. 10, pp. 4612-4624, 2012.
- [13] H. Tao, A. Kotsopoulos, J. L. Duarte and M. A. M. Hendrix, "Multi-input bidirectional DC-DC converter combining DC-link and magnetic-coupling for fuel cell systems," in *Fourtieth IAS Annual Meeting, Conference Record of the Industry Applications Conference, 2005*, Hong Kong, vol. 3, 2005, pp. 2021-2028,.
- [14] J. Zeng, W. Qiao, and L. Qu, "An isolated multiport bidirectional DC-DC converter for PV-battery-DC microgrid applications," in *2014 IEEE Energy Conversion Congress and Exposition (ECCE)*, Pittsburgh, PA, 2014, pp. 4978-4984.
- [15] Qian Z., Abdel-Rahman O. and Batarseh, "An integrated four-port DC/DC converter for renewable energy applications," *IEEE Transactions on Power Electronics*, vol. 25, no. 7, pp. 1877-1887, 2010.
- [16] W. Li, J. Xiao, Y. Zhao and X. He, "PWM Plus Phase Angle Shift (PPAS) Control Scheme for Combined Multiport DC/DC Converters," *IEEE Transactions on Power Electronics*, vol. 27, no. 3, pp. 1479-1489, 2012.
- [17] J. Zhang, H. Wu, X. Qin and Y. Xing, "PWM Plus Secondary-Side Phase-Shift Controlled Soft-Switching Full-Bridge Three-Port Converter for Renewable Power Systems," *IEEE Transactions on Industrial Electronics*, vol. 62, no. 11, pp. 7061-7072, 2015.
- [18] H. Wu, J. Zhang, X. Qin, T. Mu, and Y. Xing, "Secondary-Side-Regulated Soft-Switching Full-Bridge Three-Port Converter Based on Bridgeless Boost Rectifier and Bidirectional Converter for Multiple Energy Interface," *IEEE Transactions on Power Electronics*, vol. 31, no. 7, pp. 4847-4860, 2016.
- [19] Al-Atrash, Hussem, and Issa Bataresh, "Boost-integrated phase-shift full-bridge converter for three-port interface," *2007 IEEE Power Electronics Specialists Conference*, Orlando, FL, 2007, pp. 2313-2321.
- [20] Mira M. C., Zhang Z., Knott. A., Anderson M. A., "Analysis, Design, Modeling and control of an interleaved-boost full-bridge three-port converter for hybrid renewable energy systems," *IEEE Transactions on Power Electronics*, vol. 32, no. 2, pp. 1138-1155, 2017.
- [21] H. Wu, P. Xu, H. Hu, Z. Zhou and Y. Xing, "Multiport Converters Based on Integration of Full-Bridge and Bidirectional DC-DC Topologies for Renewable Generation Systems," *IEEE Transactions on Industrial Electronics*, vol. 61, no. 2, pp. 856-869, 2014.
- [22] P. Kolahian, H. Tarzamani, A. Nikafrooz and M. Hamzeh, "Multi-port DC-DC converter for bipolar medium voltage DC micro-grid applications," *IET Power Electronics*, vol. 12, no. 7, pp. 1841-1849, 2019.
- [23] Zhang, Zhe and Anderson, Michael, "Interleaved Boost-Half-Bridge Dual-Input DC-DC converter with a PWM plus Phase-shift control For Fuel Cell applications," *IEEE Industrial Electronics annual conference-2013 proceedings, Vienna*, 2013, pp. 1679-1684.
- [24] G. Oggier, G. O. Garcia and A. R. Oliva, "Modulation strategy to operate the dual active bridge DC-DC converter under soft switching in the whole operating range," *IEEE Transactions on Power Electronics*, vol. 26, no. 4, pp. 1228-1236, 2011.
- [25] B. J. Byen, B. H. Jeong and G. H. Choe, "Single Pulse-Width-Modulation Strategy for Dual-Active Bridge converters," *Journal of Power Electronics*, vol. 18, no. 1, pp. 137-146, 2018.